Computational and Structural Biotechnology Journal 20 (2022) 4390–4401

COMPUTATIONAL ANDSTRUCTURAL BIOTECHNOLOGY JOURNAL

journal homepage: www.elsevier.com/locate/csbj

Integrated analysis and validation reveal ACAP1 as a novel prognostic biomarker associated with tumor immunity in lung adenocarcinoma

Ning Wang [a,1], Lingye Zhu [a,1], Xiaomei Xu [a,1], Chang Yu [b,*], Xiaoying Huang [a,*]

[a] Division of Pulmonary Medicine, The First Affiliated Hospital of Wenzhou Medical University, Key Laboratory of Heart and Lung, Wenzhou, Zhejiang 325000, PR China
[b] Intervention Department, The First Affiliated Hospital of Wenzhou Medical University, Wenzhou, Zhejiang 325000, PR China

ARTICLE INFO

Article history:
Received 9 May 2022
Received in revised form 10 August 2022
Accepted 10 August 2022
Available online 13 August 2022

Keywords:
ACAP1
Lung adenocarcinoma
Prognosis
Immune infiltrates
Immunotherapy

ABSTRACT

ADP-ribosylation factor (Arf)-GTPase-activating protein (GAP) with coiled-coil, ankyrin repeat and PH domains 1 (ACAP1) has been reported to serve as an adaptor for clathrin coat complex playing a role in endocytic recycling and cellular migration. The potential role of ACAP1 in lung adenocarcinoma (LUAD) has not been yet completely defined. We performed the comprehensive analyses, including gene expression, survival analysis, genetic alteration, function enrichment, and immune characteristics. ACAP1 was remarkably downregulated in tumor tissues, and linked with the clinicopathologic features in LUAD patients. Prognostic analysis demonstrated that low ACAP1 expression was correlated with unsatisfactory overall survival (OS) and disease specific survival (DSS) in LUAD patients. Moreover, ACAP1 could be determined as a prognostic biomarker according to Cox proportional hazard model and nomogram model. We also confirmed that ACAP1 was downregulated in two LUAD cell lines, comparing to normal lung cell. Overexpression of ACAP1 caused a profound attenuation in cell proliferation, migration, invasion, and promoted cell apoptosis. Additionally, functional enrichment analyses confirmed that ACAP1 was highly correlated with T cell activation and immune response. Then, we further conducted immune landscape analyses, including single cell RNA sequencing, immune cells infiltration, and immune checkpoints. ACAP1 expression was positively associated with the infiltrating level of immune cells in TME and the expression of immune checkpoint molecules. This study first comprehensively analyzed molecular expression, clinical implication, and immune landscape features of ACAP1 in LUAD, suggesting that ACAP1 was predictive of prognosis and could serve as a potential biomarker predicting immunotherapy response for LUAD patients.

1. Introduction

Lung cancer, the most common cancer type in humans, accounts for the majority of cancer-related deaths around the world, with lung adenocarcinoma (LUAD) being the primary subtype [1,2]. Despite advancements in multimodality therapy, including surgery, chemotherapy, and radiotherapy, lung cancer is still a key point in the malignancy landscape with limited survival (5-year survival rate approximately 20 %) [3]. The development of driver genes mutations identification and targeted therapies have reformed the treatment paradigm for the patients with lung cancer [4,5]. However, only 15 to 20 % of patients with drug-sensitive mutations present clinical benefit to targeted therapies [6]. During the past of few years, immunotherapy represented by antibodies targeting immune checkpoint molecules involving programmed death receptor 1 (PD-1) and programmed

Abbreviations: ACAP1, ADP-ribosylation factor (Arf)-GTPase-activating protein (GAP) with coiled-coil, ankyrin repeat and PH domains 1; Arf6, ADP-ribosylation factor 6; CAMs, cell adhesion molecules; CI, confidence interval; DEGs, differentially expressed genes; GEFs, guanine nucleotide exchange factors; GEPIA, gene expression profiling interactive analysis; GO, gene ontology; GSEA, Gene Set Enrichment Analysis; GTEx, genotype-tissue expression; HR, hazard ratio; ICB, immune checkpoint blockade; KEGG, Kyoto encyclopedia of genes and genomes; LUAD, lung adenocarcinoma; OS, overall survival; DSS, disease specific survival; PD-1, programmed death receptor 1; PD-L1, programmed death receptor ligand 1; PPI, protein–protein interaction; qRT-PCR, quantitative reverse-transcription polymerase chain reaction; TCGA, the cancer genome atlas; TIME, tumor immune microenvironment; TIMER, tumor immune estimation resource; TME, tumor microenvironment.

* Corresponding authors.
E-mail addresses: wzmcyc@126.com (C. Yu), zjwzhxy@126.com (X. Huang).
[1] These authors share co-first authorship.

https://doi.org/10.1016/j.csbj.2022.08.026

death receptor ligand 1 (PD-L1) has been considered as a recent major breakthrough in novel therapeutic option improving lung cancer patients' survival [7,8]. T cell-mediated antitumor immunity effects can be strengthened owing to the blockage of inhibitory signals by the antibodies targeting PD-1 or PD-L1. Evidence appears that immunotherapy response is largely associated with the tumor immune microenvironment (TIME) [9,10]. Nevertheless, the sticking point that needs to be resolved in cancer immunotherapy is low response rate in patient. Consequently, there is urgent need to further investigate the intrinsic mechanism between tumor microenvironment (TME) and immunotherapy response.

ADP-ribosylation factors (Arfs), belonging to Ras-like GTP-binding proteins, perform a significant role in regulating the cellular procedure such as intracellular vesicle trafficking, cytoskeletal reorganization and Golgi structure in eukaryotic organisms [11]. ADP-ribosylation factor (Arf)-GTPase-activating protein (GAP) with coiled-coil, ankyrin repeat and PH domains 1 (ACAP1) has been reported to serve as an adaptor for clathrin coat complex exerting a role in endocytic recycling and regulate the cellular migration procedure [12,13]. According to recent research findings, the small GTPase ADP-ribosylation factor 6 (Arf6) participates in the regulation of recruiting ACAP1 to the recycling endosome [14]. A recent study has demonstrated that the protein kinase Akt serves as a co-adaptor with ACAP1 for joint participation of clathrin coat complex in endocytic recycling [15]. The potential regulation of Arf6/ACAP1 in cell migration and cytokinesis contributes to cell division, invasion and migration of cancer cells [16]. Besides, previous studies have identified that ACAP1 is connected with immune infiltration in bladder cancer [17] and ovarian cancer [18]. Yet so far, the potential biological function of ACAP1 in LUAD has not been fully elaborated.

In this study, on the basis of database analysis and experimental validation, we first elucidated the expression characteristics of ACAP1 in LUAD, and the relevance between ACAP1 expression and the clinicopathologic features in LUAD patients. In addition, the prognostic value of ACAP1 in LUAD was investigated. Gene-gene and protein–protein network and subsequent functional enrichment analyses were performed to determine the potential biological function. Finally, our research focused on the identification of the immune characteristics of ACAP1 in LUAD. Taken together, our study comprehensively identified the biological function of ACAP1 and disclosed that ACAP1 might function as a meaningful prognostic biomarker and exert a predictive effect on response to immunotherapy in LUAD.

2. Materials and methods

2.1. Data acquisition and process

RNA-sequencing and matched clinical data involving LUAD and normal tissues were acquired from The Cancer Genome Atlas (TCGA) (https://portal.gdc.cancer.gov/) and Genotype-Tissue Expression (GTEx) databases (https://www.gtexportal.org/home/index.html). After log2 transformation, the data was conducted statistical analysis using R software, and visualization via the "ggplot2" package.

2.2. Gene expression analysis based on database

We initially investigated ACAP1 expression between tumor and normal tissues across multiple cancer types via TCGA and GTEx databases. Furthermore, ACAP1 expression was assessed in LUAD tissues using Gene Expression Profiling Interactive Analysis (GEPIA) (http://gepia.cancer-pku.cn/) [19]. Meanwhile, ACAP1 expression in distinct pathological stages could be observed. In addition, the correlation analyses of ACAP1 expression with different TNM stages of LUAD patients were performed. The association between ACAP1 expression and related clinicopathologic characteristics were described via Sankey diagram accomplished by the "ggalluvial" package.

2.3. Cell culture and transfection

Human embryonic lung fibroblast lines (HELF, normal human lung cells) and human LUAD cell lines (A549 and PC-9) were purchased from Institute of Biochemistry and Cell Biology, Chinese Academy of Science (Shanghai, China). HELF and PC-9 cells were grown in high glucose Dulbecco's Modified Eagle's media (DMEM), and A549 cells were grown in F-12k culture medium. All cells were routinely cultivated in the medium mixed by 10 % fetal bovine serum (FBS), and 1 % Penicillin/Streptomycin at 37 °C in the incubator (Thermo, USA) with 5 % CO_2. To obtain ACAP1 overexpressed cell lines, the transfection was performed with plasmids using PolyFast Transfection Reagent (MCE, USA) according to manufacturer's instructions. ACAP1-pcDNA3.1 overexpression (OE) and negative control (NC) plasmids were purchased from Ruipute Biotech (Hangzhou, China). RNA and protein were harvested at 48 h after the transfection for assessing the gene expression level. In addition, related function experiments were conducted after transfection.

2.4. Quantitative reverse-transcription polymerase chain reaction

Total RNA was extracted by means of the RNA fast 200 Extraction kit (Fastagen Biotech, China), and then RNA concentration was detected using NanoDrop 2000 spectrophotometer (Thermo, USA). After reverse transcription via PrimeScript RT Master Mix (Takara, Japan), qRT-PCR was conducted using Taq Pro Universal SYBR qPCR Master Mix (Vazyme, China) via the CFX96 Real-Time System (Bio-Rad, USA). GAPDH was used for normalization. Primers were synthesized in Sangon Biotech (Shanghai, China) and the sequences were shown in Supplementary Table 1.

2.5. Western blot analysis

The total proteins were extracted according to the protocol. After quantification by BCA Protein Assay (Beyotime, China), the same amounts of denatured protein were added into per lane and separated by sodium dodecyl sulfate polyacrylamide gels (SDS-PAGE). Then, the protein was transferred onto PVDF membranes (Millipore, USA), with performed subsequent steps such as blocking, primary antibodies culture against ACAP1 (1:5000, Proteintech) and GAPDH (1:3000, Proteintech), and the secondary antibody culture according to species of primary antibodies. Finally, the expression levels of proteins were determined using enhanced chemiluminescent (NCM Biotech, China) via gel imaging system (Bio-Rad, USA).

2.6. Cell viability assay and colony formation assay

A total of 3×10^3 cells/well were plated into 96-well plates and cultured for 24, 48, 72, and 96 h, respectively. At different time points, the cells were incubated with fresh serum-free medium mixed with 10 % CCK-8 (APExBIO, USA) solution for cell viability assay. The changes in cell proliferation were assessed by measuring the absorbance at 450 nm via multifunctional microplate reader (Thermo, USA). For colony formation assay, a total of 500 cells per well were spread onto six-well plates and cultured for two weeks. The colonies were then fixed with 4 % paraformaldehyde for 30 min and stained with crystal violet (Beyotime, China)

for 20 min. Finally, the colony number was counted for statistical analysis.

2.7. Apoptosis assay

Annexin V FITC/PI apoptosis Kit (Multisciences, China) was utilized to detect cell apoptosis. The transfected cells were washed twice using cold PBS and harvested for apoptosis assay. The cells were incubated using 1 × binding buffer with FITC-Annexin V and PI for 5 min at room temperature. After incubation, the apoptosis assay was conducted via flow cytometry (Beckman, USA), and the results were processed by FlowJo V10 software.

2.8. Wound-healing assay

The wound healing assay was utilized to assess cell motility. The cells were cultured in 6-well plate, and scratched with a sterile plastic tip upon cell confluence. Following this, the cells were continued to be cultured with serum-free medium, and cell migration was evaluated at different time point. The cell migration ability was assessed by comparing the width of cell scratch.

2.9. Transwell assay

Transwell assay was conducted to evaluate the ability of the cells to migrate and invade. Briefly, cells (5×10^4 cells/well) resuspended with 200 μl serum-free medium were added into the upper chamber of the insert (Millipore) equipped with and without matrigel (BD Bioscience) for assessing the ability of cell invasion and migration, respectively. Then, 500 μl medium mixed with 10 % FBS was supplied in the lower well. After incubation for 24 h at 37 °C, the cells on the upper surface were eliminated and the cells located on the lower side of the membrane were stained by crystal violet for 20 min through fixation with 4 % paraformaldehyde for 30 min. The number of cells were counted in randomly selected three fields under the microscope (×200) for further statistical analysis.

2.10. Prognosis analysis

Overall survival (OS) and disease specific survival (DSS) analyses were conducted to determine the correlation between ACAP1 expression and LUAD patients' survival using the "survival" package. Then, we conducted the univariate and multivariate Cox regression analyses to recognize the appropriate variables for establishing a nomogram model via the "forestplot" package. Additionally, the prognostic nomogram model was constructed using the "rms" package.

2.11. Genetic alteration analysis

The genetic alteration features of ACAP1 in multiple types of cancer were observed utilizing cBioPortal platform containing multidimensional cancer genomics data (https://www.cbioportal.org/) [20,21]. In the module "Mutations", ACAP1 mutation sites could be discovered. Furthermore, somatic mutation landscape based on ACAP1 expression in LUAD was constructed using the "maftools" package.

2.12. Construction of ACAP1-interacting genes and proteins network

The ACAP1-associated gene-gene interaction network was created via the Genemania database (https://www.genemania.org). The ACAP1-associated protein–protein interaction (PPI) network was established via the STRING database (https://string-db.org/). The main parameters were as follows: "experiments" option was selected in "active interaction sources" module; "Low confidence (0.150)" option was selected in "minimum required interaction score" module; and "no more than 50 interactors" option was selected in "max number of interactors to show" module. The visualization was performed using Cytoscape (Version: 3.8.0).

2.13. Function enrichment analysis

The differentially expressed genes (DEGs) were obtained by comparing between $ACAP1^{high}$ and $ACAP1^{low}$ groups of the expression data with setting the screening criteria of adjusted $P < 0.05$ and Fold Change > 2, using the "Limma" package. Subsequently, Kyoto encyclopedia of genes and genomes (KEGG) and Gene Ontology (GO) analyses were conducted via the "ClusterProfiler" package. In addition, Gene Set Enrichment Analysis (GSEA) was applied to further investigate the significant pathways, including HALLMARK and KEGG, between $ACAP1^{high}$ and $ACAP1^{low}$ expression samples, and the most obvious signaling pathways in HALLMARK and KEGG were visualized in plots.

2.14. Immune characteristics analysis

TISCH, a comprehensive resource database, can provide a standardized data of single-cell transcriptome for exploring the heterogeneity of TME and promoting the development of tumor immunotherapy [22]. Then, we investigated the expression status of ACAP1 across multiple cell types in TME based on the two datasets (GSE131907 and GSE139555) via TISCH platform (http://tisch.comp-genomics.org/home/). TISIDB (http://cis.hku.hk/TISIDB/) [23] can be utilized to explore 28 immune cells infiltration in TME across various cancer types. The TIMER database (https://cistrome.shinyapps.io/timer/) is utilized to evaluate six immune cells infiltration in TME [24,25]. xCell [26], a novel gene signature-based algorithm, can be employed to analyze the immune cells infiltration using the "immunedeconv" package. Therefore, TISIDB, TIMER databases and xCell algorithm were utilized to estimate ACAP1-related immune cells infiltration in LUAD. Next, we evaluated the association of ACAP1 expression with the Immune Score, Stromal Score and ESTIMATE Score by Spearman correlation analysis in LUAD. Based on the level of expression, samples were divided into high and low groups, and then ssGSEA algorithm was performed to predict the score of the corresponding immune gene set of each sample, which was visualized utilizing the "ggplot2" package. Finally, we assessed the relevance between ACAP1 expression and the eight major immune checkpoint genes such as CD274, CTLA4, HAVCR2, LAG3, PDCD1, PDCD1LG2, SIGLEC15, and TIGIT.

2.15. Statistical analysis

The difference between two groups was analyzed using Student's *t* test or Wilcoxon rank sum test. Spearman rank correlation was conducted for determining the correlation between two genes expression. R software version 4.0.3 was used for all of the packages mentioned above, and $P < 0.05$ was considered statistically significant.

3. Results

3.1. Gene expression profile of ACAP1 in LUAD

We first confirmed that ACAP1 was significantly downregulated in tumor tissues comparing with the normal tissues via TCGA and GTEx database (Fig. 1A, B). Furthermore, the relevance between ACAP1 expression and clinicopathological characteristics of LUAD

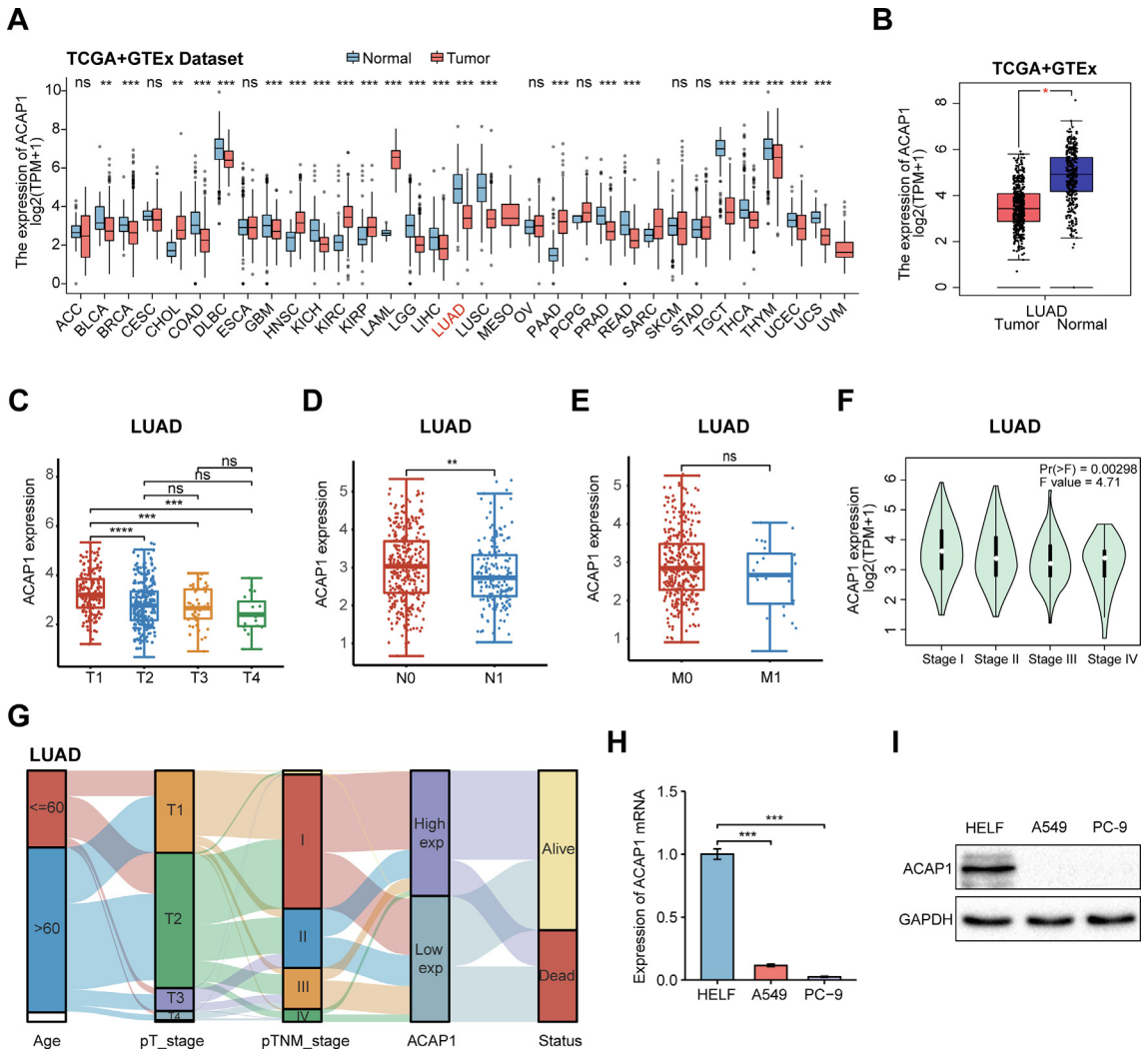

Fig. 1. The analyses of ACAP1-related expression and clinicopathologic features in LUAD. (A) The expression level of ACAP1 in normal and tumor tissues across multiple cancer types was assessed via TCGA and GTEx database. (B) The expression level of ACAP1 in LUAD was assessed via GEPIA database. (C-E) The expression level of ACAP1 was assessed in different (C) *T*-stage, (D) *N*-stage, and (E) M-stage in LUAD patients. (F) The expression level of ACAP1 was assessed in distinct pathological stages via GEPIA database. (G) The description of ACAP1 expression and the different clinicopathological features by Sankey diagram. (H, I) Validation of ACAP1 expression in normal lung cell (HELF) and LUAD cells (A549 and PC-9) by (H) qRT-PCR and (I) western blot analysis. GAPDH was used for normalization. Experimental data are acquired from three independent experiments. Statistical analysis: $^{*}P < 0.05$, $^{**}P < 0.01$, $^{***}P < 0.001$ and $^{****}P < 0.0001$.

patients were conducted according to TCGA data. The ACAP1 expression was dramatically linked with different *T*-stage (Fig. 1C) and *N*-stage (Fig. 1D) and showed no significant correlation with M-stage (Fig. 1E) for patients. Subsequently, we uncovered that ACAP1 expression was linked with the different pathological stages of LUAD patients (Fig. 1F, $P < 0.01$). The Sankey diagram displayed the distribution trend of ACAP1 expression in LUAD patients with different clinicopathological features such as age, stage, and survival status (Fig. 1G). Finally, we uncovered that the mRNA and protein level of ACAP1 were remarkably downregulated in LUAD cell lines (A549 and PC-9) with the normal cell line (HELF) as control (Fig. 1H, I).

3.2. ACAP1 was identified as an independent prognostic factor for LUAD patients

For survival analysis, LUAD patients were divided into two groups such as $ACAP1^{high}$ and $ACAP1^{low}$ based on the level of ACAP1 expression. Low ACAP1 expression was identified to be related with poor clinical outcomes in LUAD patients by means of Kaplan–Meier survival analyses (OS, $P = 0.00063$; DSS, $P = 0.013$) (Fig. 2A, B). In addition, ACAP1 and TNM-stage had been confirmed as independent prognostic factors closely related with patients' OS according to the univariate and multivariate Cox regression analyses (Fig. 2C, D). Subsequently, we constructed overall survival nomogram model to estimate 1-, 3-, and 5-year survival status and calibration curve with favorable goodness of fit ($P < 0.001$) (Fig. 2E, F).

3.3. Genetic alteration features of ACAP1 in LUAD

The alteration frequency of ACAP1 in multiple types of cancers was observed through cBioPortal, of which "Mutation" and "Deep Deletion" were mainly presented in LUAD (Fig. S1A). We then explored the types, sites and corresponding domain of the ACAP1 mutations in LUAD with "Missense" occupying the major part (Fig. S1B). The 3D structure of ACAP1 protein was exhibited in Fig. S1C (PDB ID (https://doi.org/10.2210/pdb4CKG/pdb)). Meanwhile, the somatic mutations landscape and top 10 somatic mutation genes in LUAD cohort was determined. Notably, there were

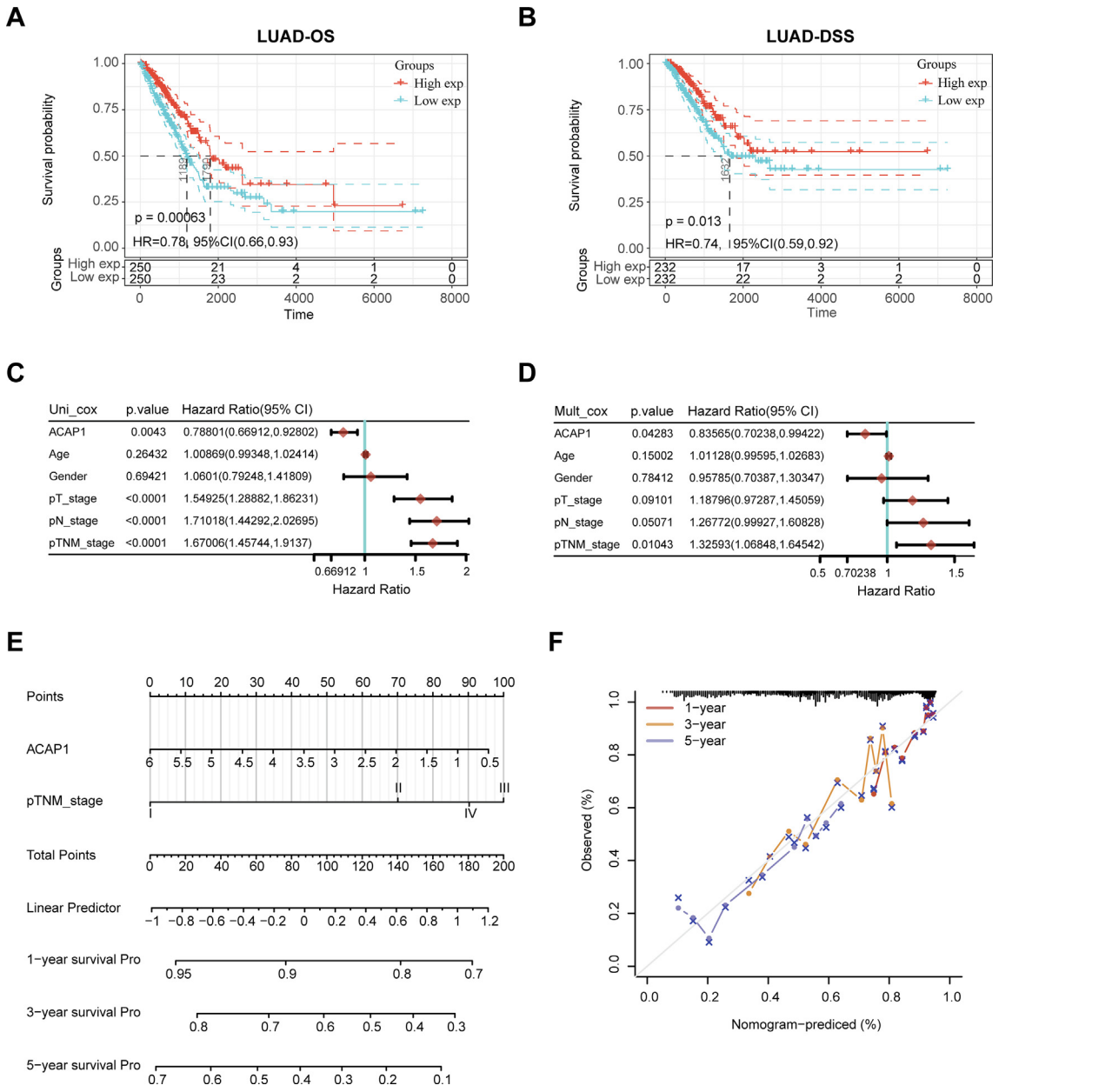

Fig. 2. Comprehensive prognosis analysis of ACAP1 expression in LUAD. (A, B) Kaplan-Meier survival curve for (A) OS and (B) DSS. (C) The univariate and (D) multivariate Cox regression analyses of ACAP1 expression and corresponding clinical features. (E) Construction of the nomogram model for LUAD. The "total points" can be obtained by summing the respective "points" values of the four variables (ACAP1 expression and pTNM_stage) and then the 1-, 3-, 5-year survival status of patients can be predicted. (F) Calibration curve for the overall survival nomogram model.

more somatic mutations in LUAD patients with low ACAP1 expression (Fig. S1D).

3.4. Inhibitory effects of ACAP1 upregulation on cell proliferation, migration and invasion in LUAD

Since ACAP1 was considerably down-regulated in A549 and PC-9 cell lines, we explored whether ACAP1 overexpression exerted an influence on tumor cells. We carried out a series of experiments to further determine the potential biological function of ACAP1 in LUAD cells. Firstly, A549 and PC-9 cell lines were transfected with ACAP1 overexpression plasmid or a control vector, and ACAP1 was successfully upregulated in cells validated at mRNA and protein level respectively (Fig. 3A, B). Then, overexpression of ACAP1 in A549 and PC-9 cell lines resulted in significantly inhibitory effects on cell proliferation (Fig. 3C) and the cell clone formation (Fig. 3D). Additionally, the results of flow cytometry assay revealed that the percentage of cell apoptosis was increased in A549 and PC-9 cells with ACAP1 upregulation (Fig. 3E). Finally, wound healing assay indicated that the migration ability of LUAD cells was suppressed after ACAP1 overexpression (Fig. 4A). Meanwhile, ACAP1 upregulation resulted in the restraining effect on cell migration and invasion (Fig. 4B).

3.5. Construction of ACAP1-interacted genes and proteins network, and enrichment analysis

The ACAP1-related gene-gene interaction network was constructed via Genemania database. This network exhibited that top 20 most frequently altered genes were significantly linked with

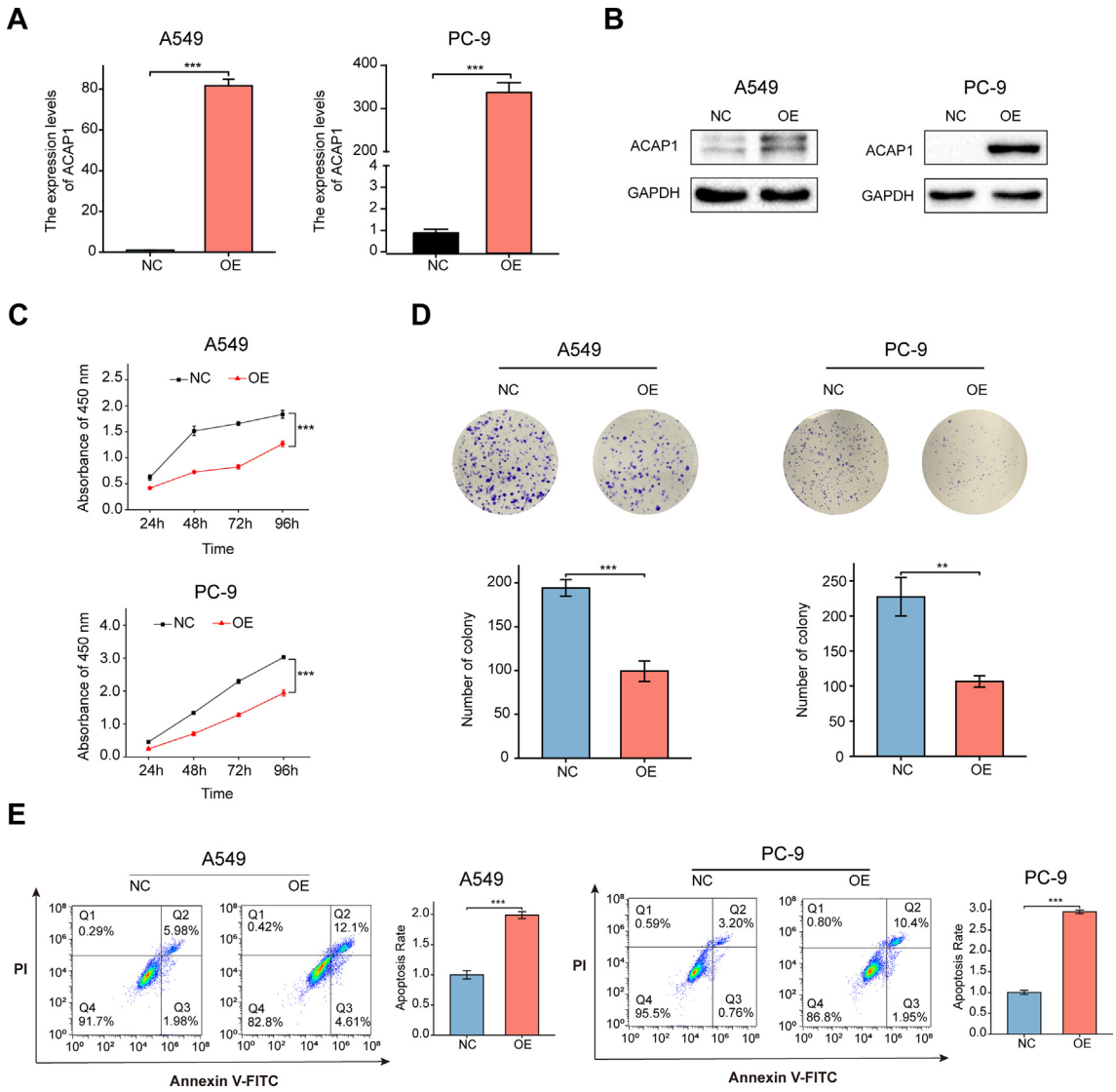

Fig. 3. Function analysis of ACAP1 upregulation in LUAD cells. (A, B) Validation of ACAP1 expression in ACAP1 overexpression (OE) and negative control (NC) cells (A549 and PC-9) at the (A) mRNA and (B) protein level, respectively. GAPDH was used for normalization. (C) The cell proliferation ability of A549 and PC-9 with overexpressing ACAP1 was examined by CCK-8 assay. (D) Effect of ACAP1 upregulation on the colony formation in A549 and PC-9 cells. (E) The apoptosis analysis of A549 and PC-9 with overexpressing ACAP1 was performed by flow cytometry. Experimental data are acquired from three independent experiments. Statistical analysis: $^{**}P < 0.01$ and $^{***}P < 0.001$.

ACAP1 (Fig. 5A). The PPI network of ACAP1-interacting proteins was formed utilizing STRING and visualized by Cytoscape (Fig. 5B). Subsequently, we conducted DEGs, function enrichment such as KEGG and GO analyses for further exploring and elucidating the potential biological role of ACAP1 in LUAD. First, differential gene expression analysis was performed between $ACAP1^{high}$ and $ACAP1^{low}$ expression samples. The volcano plot displayed that there were 228 differentially expressed genes including 226 upregulated genes and 2 downregulated genes (Fig. 5C). The detailed genes information can be observed in the Supplementary Material. Then, the heatmap of the differential gene expression was constructed based on hierarchical clustering analysis (Fig. 5D). Furthermore, KEGG enrichment analysis confirmed that upregulated DEGs mainly connected with cell adhesion molecules (CAMs), cytokine – cytokine receptor interaction, Th1, Th2 and Th17 cell differentiation, and hematopoietic cell lineage (Fig. 5E). Simultaneously, the results of GO enrichment analysis determined that upregulated DEGs highly correlated with T cell activation, immune response, leukocyte proliferation and regulation of cell–cell adhesion (Fig. 5F).

Furthermore, GSEA analysis was conducted to investigate the potential signaling pathways in HALLMARK and KEGG from high and low ACAP1 expression samples (Fig. S2A-D). Results of the function enrichment of HALLMARK terms revealed that high ACAP1 expression was linked with allograft rejection, apoptosis, complement, IL2-STAT5, IL6-JAK-STAT3, KRAS, TNFα signaling, inflammatory response, and interferon response. KEGG terms demonstrated that high ACAP1 expression was mainly involving in allograft rejection, asthma, and so on.

3.6. Immune characteristics analysis of ACAP1 in LUAD

Firstly, we performed the single cell RNA sequencing data analysis to explore the expression and distribution of ACAP1 in TME according to LUAD database. The results indicated that the expression of ACAP1 was mainly distributed in immune cell types in TME based on GSE131907 and GSE139555 (Fig. 6A-C). TIME was largely

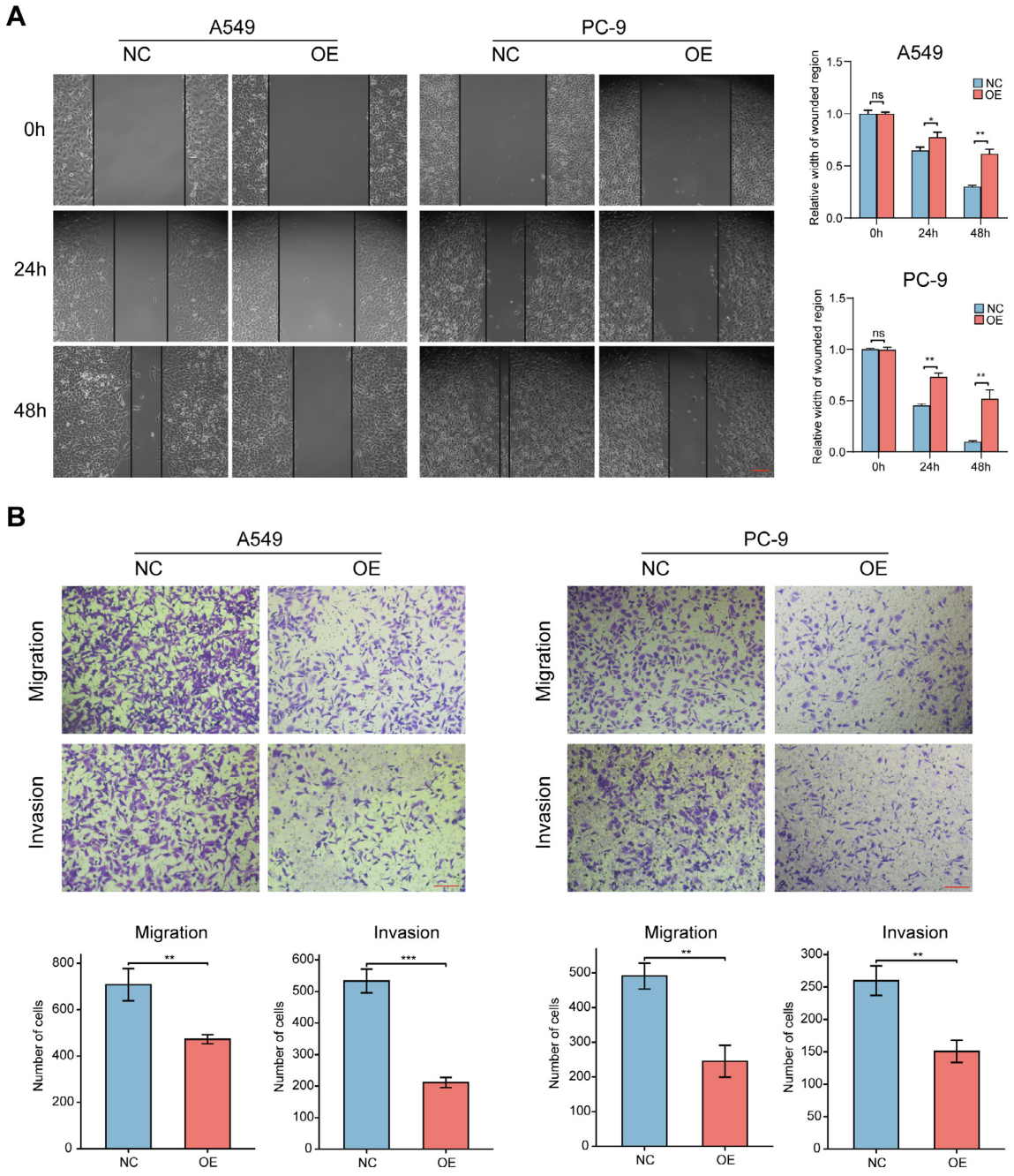

Fig. 4. Effect of ACAP1 upregulation on the migration and invasion of LUAD cells. (A) The wound healing assay showing the inhibition effects of ACAP1 overexpression on cell migration. (B) Transwell assay showing the inhibition effects of ACAP1 overexpression on cell migration and invasion. Experimental data are acquired from three independent experiments. Statistical analysis: $^{*}P < 0.05$, $^{**}P < 0.01$, $^{***}P < 0.001$ and ns, no significance.

affected by the infiltrating tumor components, which was one of the key determinants for the outcome of tumor immunotherapy [27]. We then focused on the ACAP1-related immune characteristics in LUAD. We uncovered ACAP1-related immune infiltration landscape of 28 immune cells in multiple cancers including LUAD via TISIDB database (Fig. S3A). Notably, there was a significant correlation of ACAP1 expression with a majority of the immune cells in LUAD (Fig. S3B-M) (cor > 0.5 displayed). Moreover, we assessed the immune cells infiltration level utilizing the TIMER platform and xCell algorithms in LUAD. There was a relevance between high ACAP1 expression and a low tumor purity and high immune cells infiltration in TME based on TIMER database (Fig. 7A). Meanwhile, the consistent result was obtained via xCell analysis (Fig. 7B).

Next, we discovered that there were positive correlation of ACAP1 expression with Immune Score, Stromal Score and ESTIMATE Score in LUAD (Fig. 7C). Notably, most of the 28 immune cell types exhibited significantly higher immune score in ACAP1 high expression group, which revealed that ACAP1 was closely related with immune infiltration in LUAD (Fig. 7D). Additionally, we assessed the potential relevance between ACAP1 expression and immune checkpoint genes. Significantly, the major eight immune checkpoint genes were all upregulated in LUAD patients with high ACAP1 expression (Fig. 8A). Specifically, there was a consistently positive relevance between ACAP1 expression and the major eight immune checkpoint genes (Fig. 8B-I).

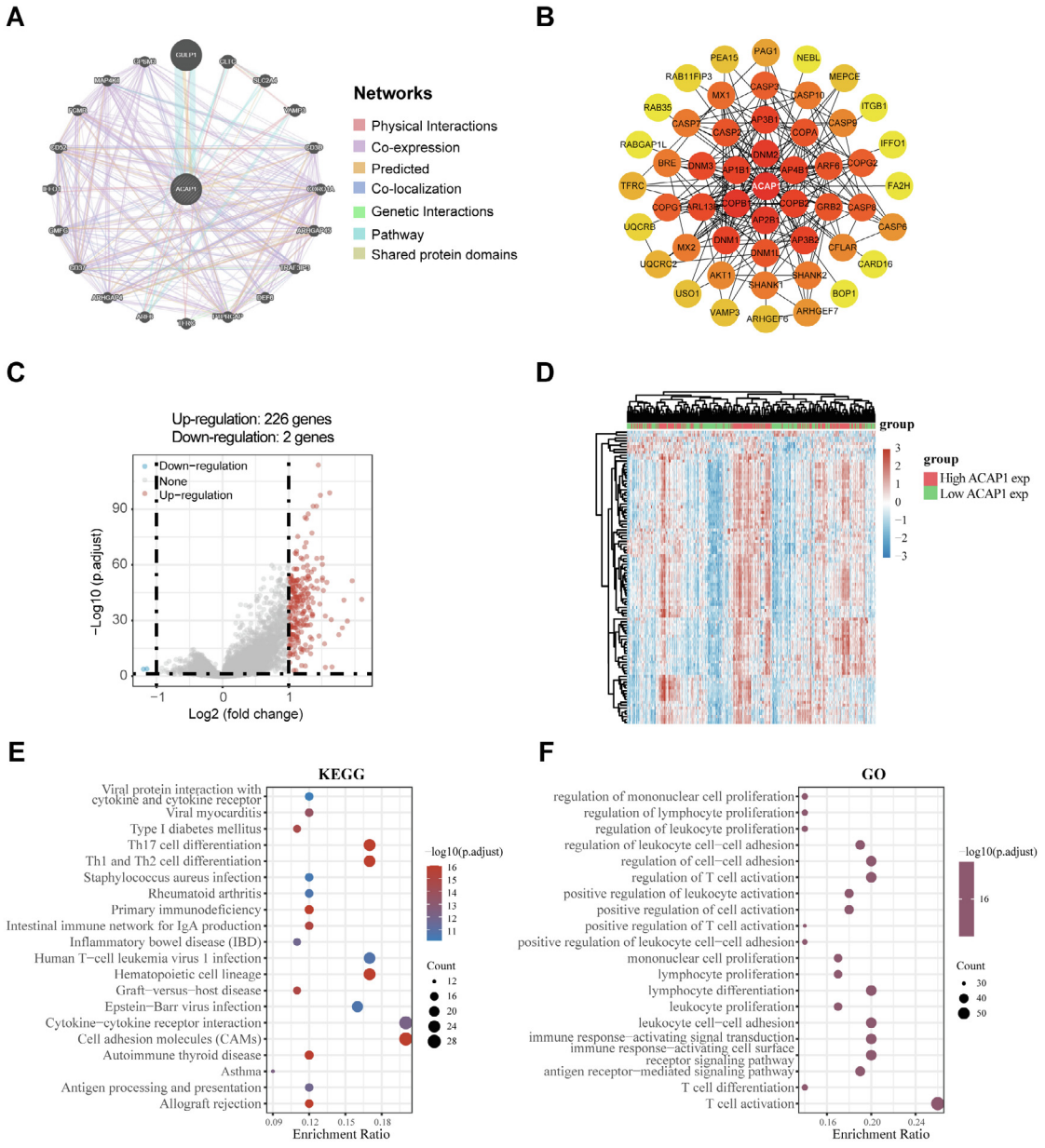

Fig. 5. Construction of ACAP1-interacted gene-gene and protein–protein network, and function enrichment analysis. (A) Construction of gene-gene network based on Genemania. (B) Construction of PPI network based on STRING. (C) Volcano plot of the differentially expressed genes between the ACAP1^{high} and ACAP1^{low} groups in LUAD. (D) Expression heatmap of screened ACAP1-associated DEGs. (E) KEGG and (F) GO enrichment analysis of upregulated DEGs in LUAD.

4. Discussion

The incidence and cancer-related death rates of lung cancer have already exceeded those of all other cancers in the world. Early diagnosis of lung cancer is challenging and late diagnosis is the primary cause of formidable death rates in the patients with lung cancer. It is vital to investigate the underlying molecular mechanisms of tumor development and progression contributing to accurately predicting and improving patients' prognosis. In the present study, we first explored the potential biological function of ACAP1 identified as a novel biomarker in LUAD. ACAP1 was remarkably downregulated in tumor tissues comparing with normal tissues, and we also conducted qRT-PCR and Western blot to validate the result.

ACAP1 expression was associated with clinicopathological characteristics of LUAD patients. Furthermore, Kaplan-Meier survival analyses (OS and DSS) revealed that LUAD patients with low ACAP1 expression presented a relatively high mortality risk than those with high expression, suggesting ACAP1 could be considered as a potential prognostic biomarker in LUAD. The univariate and multivariate Cox regression analyses and nomogram model further confirmed that ACAP1 was independently predictive of the clinical outcomes of LUAD patients. High ACAP1 expression was associated with better survival of the patients with LUAD. Taken together these data suggest that ACAP1 may have an anti-tumor effect. Consequently, we performed a series of experiments to further determine the influence of ACAP1 overexpression on tumor cells. We found that overexpression of ACAP1 in A549 and PC-9 cell lines resulted in significant restraining effect on cell proliferation, migration, invasion, and promoted cell apoptosis. These results provided evidence to validate the tumor suppressive role of ACAP1,

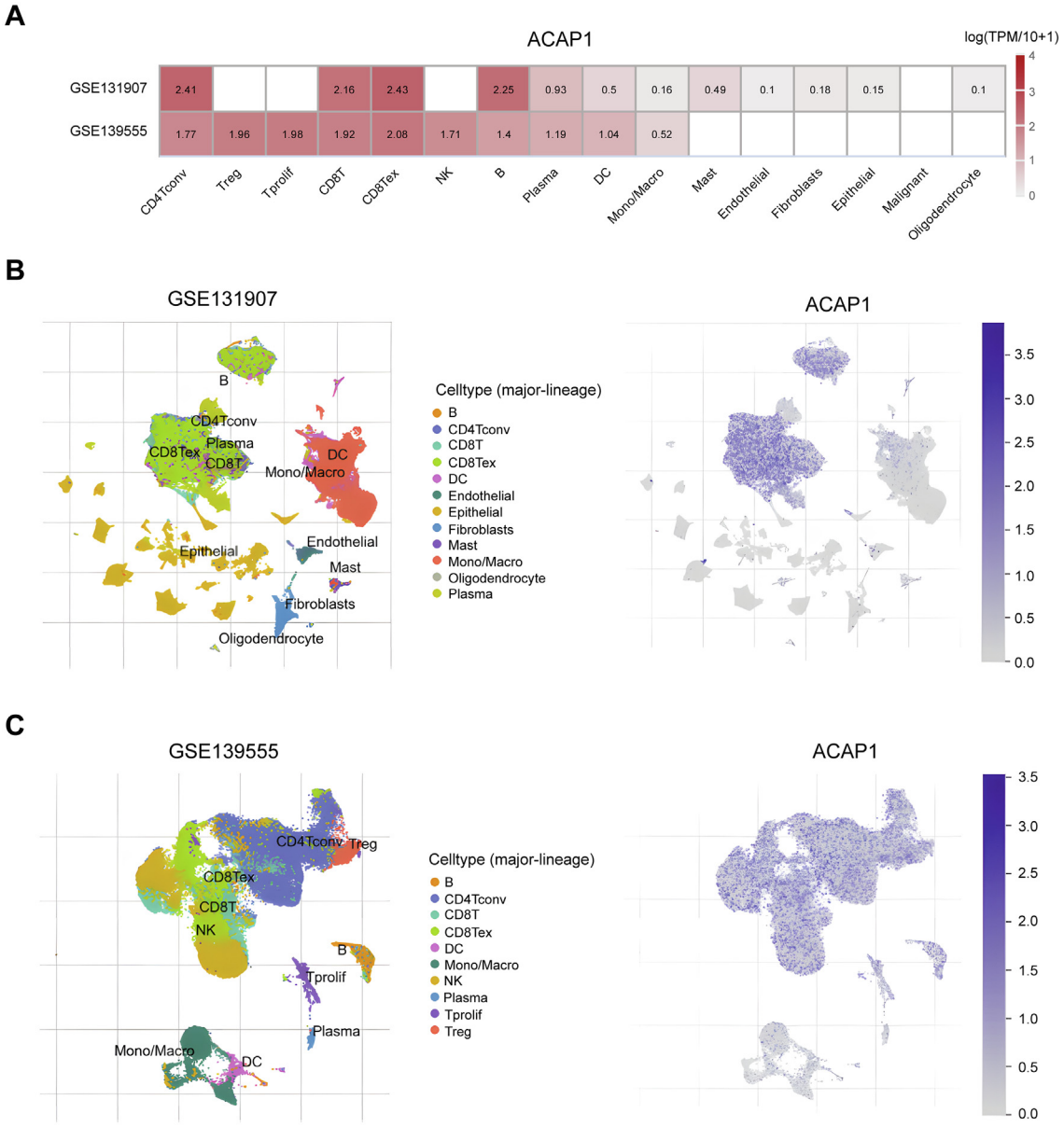

Fig. 6. Single-cell transcriptome analysis of ACAP1 expression distribution in different cell types in tumor microenvironment. (A) The correlation of ACAP1 expression with cell types in GSE131907 and GSE139555 datasets. (B, C) The expression status of ACAP1 in different cell types based on (B) GSE131907 and (C) GSE139555 dataset.

which was consistent with good prognosis of the patients with high ACAP1 expression.

To explore the potential function of ACAP1 in LUAD, we performed function enrichment analyses, including GO, KEGG, and GSEA. The results suggested that ACAP1 was significantly correlated with T cell activation and immune response. Hence, we further investigated the potential association of ACAP1 expression with tumor immune microenvironment in LUAD.

Due to the continuous and in-depth research on the mechanism of TME, immunotherapy has been considered as one of the greatest progresses and breakthroughs in cancer treatment and opened up a new avenue of cancer treatment. In particular, immune checkpoint blockade (ICB) therapy targeting tumor immune suppression pathway has been viewed as a novel paradigm shift. The application of antibodies targeting immune checkpoint molecules have confirmed to be an effective strategy for cancer therapy [28]. Besides, immune cells infiltration in TME also exerts a vital role in anti-tumor immunotherapy. Numerous studies have revealed that patients with *T*-cell-infiltration present better response to ICB therapy than those with non-*T*-cell-infiltration [29,30]. Consequently, current research concludes that the presence of tumor-infiltrating lymphocytes in TME and the expression of PD-L1 on tumor cells can be deemed as predictors of positive response to immune therapy [31].

We further detected the underlying evidence disclosing the relevance between ACAP1 expression and immune cell infiltration and immune checkpoint molecules in the patients with LUAD. High ACAP1 expression was consistent with high immune infiltration in TME base on TISIDB, TIMER, and xCell. Considering the high levels of immune cells infiltration in TME in LUAD patients with high ACAP1 expression, tumor cells might adaptively upregulate the expression of multiple immune checkpoints to cope with the changes of microenvironment. Subsequently, we conducted the correlation analysis of ACAP1 expression with eight major immune checkpoints. Interestingly, there exerted a significantly positive association between ACAP1 and immune checkpoint genes expres-

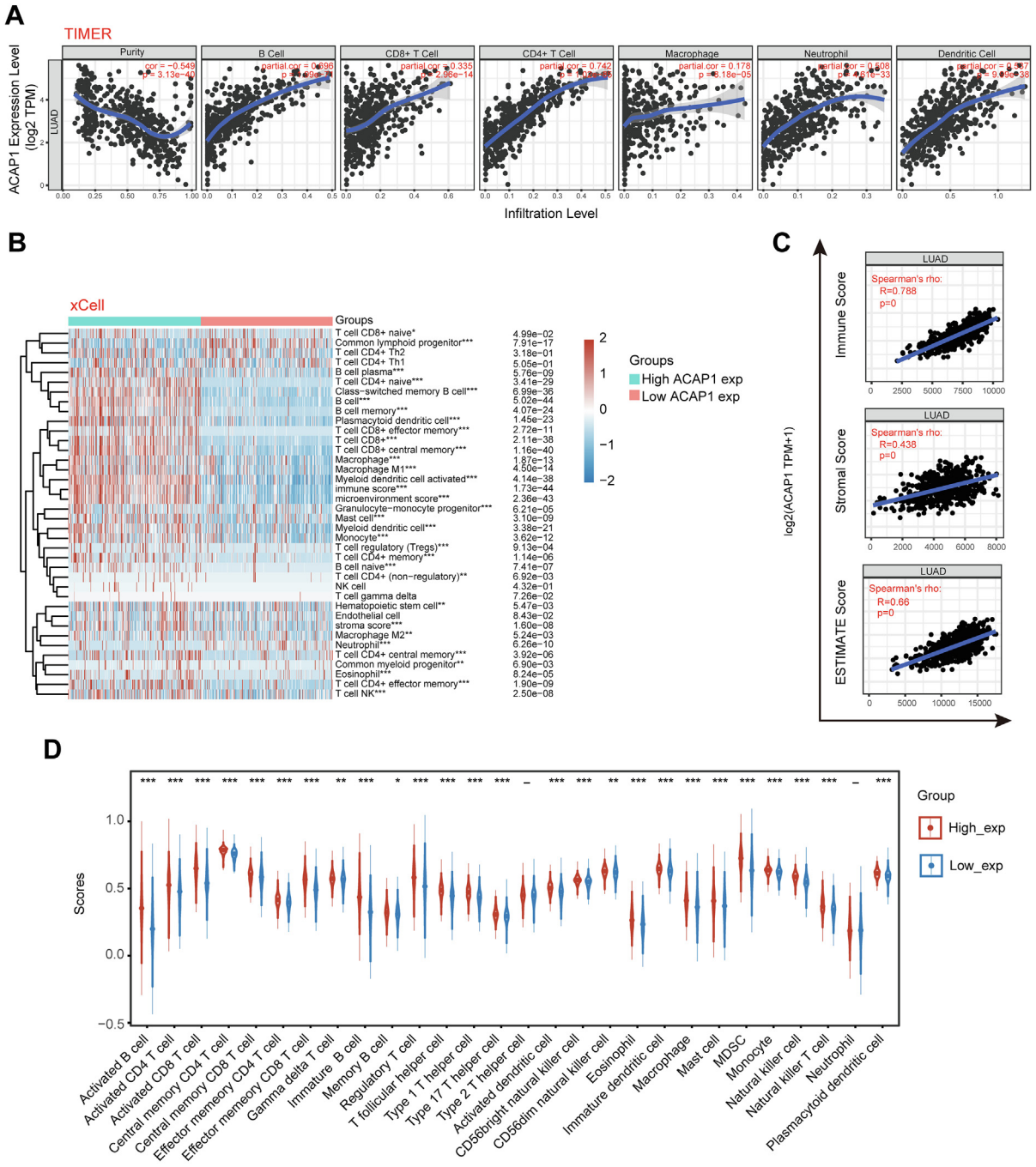

Fig. 7. The relevance between ACAP1 expression and immune cells infiltration. (A) The relevance between ACAP1 expression and immune cells infiltration in LUAD via TIMER. (B) Heatmap of the relevance between ACAP1 expression and immune cells infiltration in LUAD via xCell. (C) Correlation of ACAP1 expression with Immune Score, Stromal Score, and ESTIMATE Score in LUAD. (D) ACAP1-related immune score of 28 immune cell types in LUAD. Statistical analysis: $^{*}P < 0.05$, $^{**}P < 0.01$ and $^{***}P < 0.001$.

sion in LUAD. This result also supported our previous view. In this case, immunotherapy that blocking immune checkpoints might achieve potent antitumor effects. These results further illustrated the close relevance between ACAP1 and tumor immune, which implied that ACAP1 could be regarded as a novel potential biomarker predicting the response to immunotherapy in LUAD patients.

In conclusion, this study contributed to raising the awareness of the relationship between ACAP1 and lung adenocarcinoma from clinical and molecular immune aspects. By analyzing the results of molecular expression, clinical implication, and immune landscape features of ACAP1 in LUAD, we uncovered that ACAP1 was not only downregulated in LUAD, but also positively correlated with the prognosis of patients. Additionally, ACAP1 expression was closely associated with immune infiltrates and immune checkpoints, which made a case for the establishment of ACAP1 as a predictor of immunotherapeutic response for patients with lung adenocarcinoma.

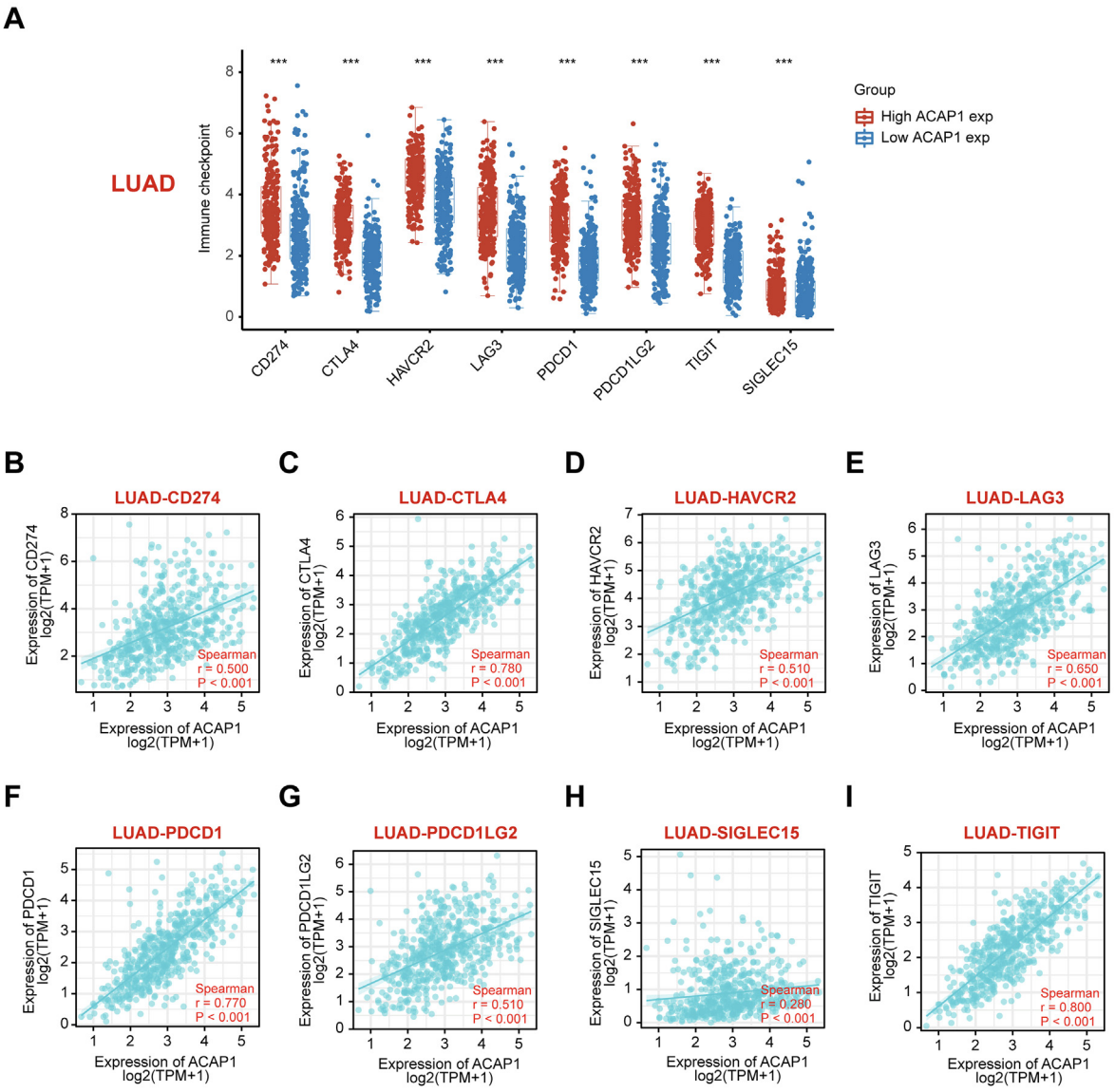

Fig. 8. The relevance between ACAP1 expression and immune checkpoint genes. (A) The expression distribution of immune checkpoint genes in ACAP1^{high} and ACAP1^{low} groups. (B–I) Correlation analysis of ACAP1 expression with immune checkpoint genes, including (B) CD274, (C) CTLA4, (D) HAVCR2, (E) LAG3, (F) PDCD1, (G) PDCD1LG2, (H) SIGLEC15, and (I) TIGIT. Statistical analysis: ***$P < 0.001$.

Funding

The study was supported by the project of Wenzhou Science and Technology Bureau (H2020010).

Author contributions

Huang XY and Yu C contributed to the design of this work. Wang N, Zhu LY and Xu XM performed the experiments, data analysis, and figure generation. Wang N wrote a draft and Huang XY revised the manuscript. All authors approved the submitted version of the manuscript.

Declaration of Competing Interest

The authors declare that they have no known competing financial interests or personal relationships that could have appeared to influence the work reported in this paper.

Appendix A. Supplementary data

Supplementary data to this article can be found online at https://doi.org/10.1016/j.csbj.2022.08.026.

References

[1] Sung H, Ferlay J, Siegel RL, et al. Global cancer statistics 2020: GLOBOCAN estimates of incidence and mortality worldwide for 36 cancers in 185 countries. CA Cancer J Clin 2021;71(3):209–49.
[2] Jin C, Lagoudas GK, Zhao C, et al. Commensal microbiota promote lung cancer development via γδ T cells. Cell 2019;176(5):998–1013.e16.
[3] Brody H. Lung cancer. Nature 2020;587(7834):S7.
[4] Aggarwal C, Thompson JC, Black TA, et al. Clinical implications of plasma-based genotyping with the delivery of personalized therapy in metastatic non-small cell lung cancer. JAMA Oncol 2019;5(2):173–80.
[5] Drilon A, Bergagnini I, Delasos L, et al. Clinical outcomes with pemetrexed-based systemic therapies in RET-rearranged lung cancers. Ann Oncol 2016;27(7):1286–91.

[6] Sarode P, Zheng X, Giotopoulou GA, et al. Reprogramming of tumor-associated macrophages by targeting β-catenin/FOSL2/ARID5A signaling: A potential treatment of lung cancer. Sci Adv 2020;6(23):eaaz6105.
[7] Berner F, Bomze D, Diem S, et al. Association of checkpoint inhibitor-induced toxic effects with shared cancer and tissue antigens in non-small cell lung cancer. JAMA Oncol 2019;5(7):1043–7.
[8] Toki MI, Mani N, Smithy JW, et al. Immune marker profiling and programmed death ligand 1 expression across NSCLC mutations. J Thorac Oncol 2018;13(12):1884–96.
[9] Binnewies M, Roberts EW, Kersten K, et al. Understanding the tumor immune microenvironment (TIME) for effective therapy. Nat Med 2018;24(5):541–50.
[10] Zeng D, Li M, Zhou R, et al. Tumor microenvironment characterization in gastric cancer identifies prognostic and immunotherapeutically relevant gene signatures. Cancer Immunol Res 2019;7(5):737–50.
[11] Feng HP, Cheng HY, Hsiao TF, et al. ArfGAP1 acts as a GTPase-activating protein for human ADP-ribosylation factor-like 1 protein. FASEB J 2021;35(4):e21337.
[12] Li J, Ballif BA, Powelka AM, Dai J, Gygi SP, Hsu VW. Phosphorylation of ACAP1 by Akt regulates the stimulation-dependent recycling of integrin beta1 to control cell migration. Dev Cell 2005;9(5):663–73.
[13] Dai J, Li J, Bos E, et al. ACAP1 promotes endocytic recycling by recognizing recycling sorting signals. Dev Cell 2004;7(5):771–6.
[14] Li J, Peters PJ, Bai M, et al. An ACAP1-containing clathrin coat complex for endocytic recycling. J Cell Biol 2007;178(3):453–64.
[15] Hsu JW, Bai M, Li K, et al. The protein kinase Akt acts as a coat adaptor in endocytic recycling. Nat Cell Biol 2020;22(8):927–33.
[16] Rueckert C, Haucke V. The oncogenic TBC domain protein USP6/TRE17 regulates cell migration and cytokinesis. Biol Cell 2012;104(1):22–33.
[17] Pan S, Zhan Y, Chen X, Wu B, Liu B. Bladder cancer exhibiting high immune infiltration shows the lowest response rate to immune checkpoint inhibitors. Front Oncol 2019;9:1101.
[18] Zhang J, Zhang Q, Zhang J, Wang Q. Expression of ACAP1 is associated with tumor immune infiltration and clinical outcome of ovarian cancer. DNA Cell Biol 2020;39(9):1545–57.
[19] Tang Z, Li C, Kang B, Gao G, Li C, Zhang Z. GEPIA: a web server for cancer and normal gene expression profiling and interactive analyses. Nucleic Acids Res 2017;45(W1):W98–W102.
[20] Cerami E, Gao J, Dogrusoz U, et al. The cBio cancer genomics portal: an open platform for exploring multidimensional cancer genomics data. Cancer Discov 2012;2(5):401–4.
[21] Gao J, Aksoy BA, Dogrusoz U, et al. Integrative analysis of complex cancer genomics and clinical profiles using the cBioPortal. Sci Signal 2013;6(269):pl1.
[22] Sun D, Wang J, Han Y, et al. TISCH: a comprehensive web resource enabling interactive single-cell transcriptome visualization of tumor microenvironment. Nucleic Acids Res. 2021. 49(D1): D1420-D1430.
[23] Ru B, Wong CN, Tong Y, et al. TISIDB: an integrated repository portal for tumor-immune system interactions. Bioinformatics 2019;35(20):4200–2.
[24] Li T, Fan J, Wang B, et al. TIMER: A Web Server for Comprehensive Analysis of Tumor-Infiltrating Immune Cells. Cancer Res. 2017. 77(21): e108-e110.
[25] Li B, Severson E, Pignon JC, et al. Comprehensive analyses of tumor immunity: implications for cancer immunotherapy. Genome Biol 2016;17(1):174.
[26] Aran D, Hu Z, Butte AJ. xCell: digitally portraying the tissue cellular heterogeneity landscape. Genome Biol 2017;18(1):220.
[27] Fridman WH, Zitvogel L, Sautès-Fridman C, Kroemer G. The immune contexture in cancer prognosis and treatment. Nat Rev Clin Oncol 2017;14(12):717–34.
[28] Pfirschke C, Engblom C, Rickelt S, et al. Immunogenic chemotherapy sensitizes tumors to checkpoint blockade therapy. Immunity 2016;44(2):343–54.
[29] Gajewski TF, Schreiber H, Fu YX. Innate and adaptive immune cells in the tumor microenvironment. Nat Immunol 2013;14(10):1014–22.
[30] Chiu DK, Tse AP, Xu IM, et al. Hypoxia inducible factor HIF-1 promotes myeloid-derived suppressor cells accumulation through ENTPD2/CD39L1 in hepatocellular carcinoma. Nat Commun 2017;8(1):517.
[31] Oweida A, Hararah MK, Phan A, et al. Resistance to radiotherapy and PD-L1 blockade is mediated by TIM-3 upregulation and regulatory T-cell infiltration. Clin Cancer Res 2018;24(21):5368–80.